

**1 A novel MARV glycoprotein-specific antibody with potentials of broad-spectrum**  
**2 neutralization to filovirus**

3 Running title: An anti-filovirus antibody fused with NPC2

4 Yuting Zhang<sup>1,2†</sup>, Min Zhang<sup>1†</sup>, Haiyan Wu<sup>1†</sup>, Xinwei Wang<sup>1,2†</sup>, Hang Zheng<sup>1,2</sup>,  
 5 Junjuan Feng<sup>1,2</sup>, Jing Wang<sup>1</sup>, Longlong Luo<sup>1</sup>, He Xiao<sup>1</sup>, Chunxia Qiao<sup>1</sup>, Xinying Li<sup>1</sup>,  
 6 Yuanqiang Zheng<sup>2</sup>, Weijin Huang<sup>3</sup>, Youchun Wang<sup>3</sup>, Yi Wang<sup>4\*</sup>, Yanchun Shi<sup>2\*</sup>,  
 7 Jiannan Feng<sup>1\*</sup>, Guojiang Chen<sup>1\*</sup>

8 <sup>1</sup>State Key Laboratory of Toxicology and Medical Countermeasures, Institute of  
 9 Pharmacology and Toxicology, Beijing, China

10 <sup>2</sup>Inner Mongolia Key Lab of Molecular Biology, School of Basic Medical Sciences,  
 11 Inner Mongolia Medical University, Hohhot, China

12 <sup>3</sup>Division of HIV/AIDS and Sex-transmitted Virus Vaccines, National Institutes for  
 13 Food and Drug Control, Beijing, China

14 <sup>4</sup>Department of Hematology, Fifth Medical Center of Chinese PLA General Hospital,  
 15 Beijing, China

16 \*Address correspondence to Yi Wang, yk091023@163.com; Yanchun Shi,  
 17 ycs5388@163.com; Jiannan Feng, fengjiannan1970@qq.com or Guojiang Chen,  
 18 jyk62033@163.com.

19 †These authors contributed equally to this work

20

## 21    **Abstract**

22    Marburg virus (MARV) is one of the filovirus species that causes a deadly  
 23    hemorrhagic fever in humans, with mortality rates up to 90%. Neutralizing antibodies  
 24    represent ideal candidates to prevent or treat virus disease. However, no antibody has  
 25    been approved for MARV treatment to date. In this study, we identified a novel  
 26    human antibody named AF-03 that targeted MARV glycoprotein (GP). AF-03  
 27    possessed a high binding affinity to MARV GP and showed neutralizing and  
 28    protective activities against the pseudotyped MARV in vitro and in vivo.  
 29    Epitope identification, including molecular docking and experiment-based analysis of  
 30    mutated species, revealed that AF-03 recognized the Niemann-Pick C1 (NPC1)  
 31    binding domain within GP1. Interestingly, we found the neutralizing activity of  
 32    AF-03 to pseudotyped Ebola viruses (EBOV, SUDV, and BDBV) harboring cleaved  
 33    GP instead of full-length GP. Furthermore, NPC2-fused AF-03 exhibited neutralizing  
 34    activity to several filovirus species and EBOV mutants via binding to CI-MPR. In  
 35    conclusion, this work demonstrates that AF-03 represents a promising therapeutic  
 36    cargo for filovirus-caused disease.

37    **Keywords** Marburg, glycoprotein, neutralizing antibody, NPC1, filovirus, NPC2

38

39

## 40 Introduction

41 Filoviruses are a nonsegmented negative-sense RNA viruses, comprised of six  
 42 genera, Ebolavirus, Marburgvirus, Cuevavirus, Striavirus, Thamnovirus and a  
 43 recently discovered sixth genus, Dianlovirus<sup>1-3</sup>. The Marburgvirus genus consists of  
 44 Marburg virus (MARV) and Ravn virus (RAVN)<sup>1,4,5</sup>. The former includes three  
 45 strains-- Uganda, Angola and Musoke. The Ebola virus genus includes six distinct  
 46 species Zaire Ebola virus (EBOV), Bundibugyo virus (BDBV), Sudan virus (SUDV),  
 47 Reston virus (RESTV), Taii Forest virus (TAFV) and Bombali virus (BOMV), the  
 48 first three of which cause severe hemorrhagic fevers<sup>6,7</sup>. The genus Cuevavirus  
 49 (Lloviu virus, LLOV) was isolated from *Miniopterus schreibersii* bats in Spain and  
 50 Hungary and potently infected monkey and human cells<sup>8,9</sup>. The genus Měnglà virus  
 51 (MLAV) was discovered in the liver of a bat from Mengla, Yunnan, China in 2019.  
 52 So far, only an almost complete RNA sequence of the viral genome is available, there  
 53 are no viable MLAVs isolated.<sup>10</sup> MARV and EBOV infect humans and non-human  
 54 primates, causing Marburg virus disease (MVD) and EBOV virus disease (EVD) with  
 55 an incubation period of 2-21 days<sup>11</sup>. The symptoms of MVD include severe headache  
 56 and high fever rapidly within 5 days of the onset of symptoms, followed by diarrhea  
 57 and vomiting, leading to up to 90% fatality rate<sup>11</sup>. MARV and EBOV have a high  
 58 potential to cause a public health emergency.

59 Glycoprotein (GP) on the surface of filoviruses is a type I transmembrane protein  
 60 and consists of GP1 and GP2 subunits<sup>12,13</sup>. It is inserted into the virus envelope in the  
 61 form of homotrimeric spikes<sup>14</sup> and is responsible for virus attachment and entry. The

62 furin cleaves Marburg GP at the amino acid 435 into two subunits, GP1 and GP2,  
63 which remains linked by a disulfide bond<sup>15</sup>. GP1 contains a receptor binding domain  
64 (RBD), a glycan cap, and a heavily glycosylated mucin-like domain (MLD), which  
65 mediates binding to entry factors and receptors<sup>16</sup>. GP2 has a partial MLD, a  
66 transmembrane domain for viral anchoring to the envelop surface, and a fusion  
67 peptide required for the fusion of virus and cell membranes<sup>17-19</sup>. In the Ebola virus,  
68 the furin cleavage site is located at residue 501 and the entire MLD is attached to the  
69 GP1 subunit<sup>20</sup>. Marburg virus contains 66 amino acids on GP2 that are absent from  
70 the Ebola virus MLD, and are called "wings" due to their outward projection and  
71 flexibility<sup>17</sup>.

72 Currently, GP is a major target for antibodies validated in filovirus-infected  
73 animals and clinical trials because it is exposed on the surface of the virus and plays a  
74 key role in viral entry<sup>21</sup>. Filoviruses initially enter cells by endocytosis<sup>22,23</sup>. Once  
75 inside the endosome, GP is cleaved by host cathepsins and glycan cap and MLD are  
76 removed, enabling GP to bind to the Niemann-Pick C1 (NPC1) receptor<sup>24,25</sup>.  
77 Interestingly, Ebola virus entry requires cathepsin B cleavage<sup>26</sup>, which is redundant  
78 for Marburg virus entry<sup>27,28</sup>. Hashiguchi et al. propose that the receptor binding  
79 domain is masked by glycan cap and MLD in the Ebola virus, whereas it is partially  
80 exposed in the Marburg virus<sup>16</sup>.

81 To date, there is no licensed treatment or vaccine for Marburg infection. Herein,  
82 we utilized phage display technology to screen an antibody in a well-established  
83 antibody library<sup>29,30</sup> and obtained a novel human antibody with prominent neutralizing

84 activity. Furthermore, NPC2 fusion at the N terminus of the light chain of this  
85 antibody renders broad-spectrum inhibition of cell entry of filovirus species and  
86 mutants.  
87

## 88 **Materials and methods**

### 89 Cell lines and plasmids

90 Human embryonic kidney cells HEK293T and human hepatoma cells Huh7 were  
 91 purchased from ATCC. These cell lines were cultured in Dulbecco's modified Eagle's  
 92 medium (DMEM) (Gibco, 11965e092) supplemented with 100 units/ml penicillin,  
 93 100 units/ml streptomycin (Gibco, 15140) and 10% fetal bovine serum (Gibco, 10099)  
 94 in a humidified atmosphere (5% CO<sub>2</sub>, 95% air) at 37°C. ExpiCHO-S cells were  
 95 purchased from Gibco and cultured in ExpiCHO™ Expression Medium (Gibco,  
 96 A29100) in a humidified atmosphere (8% CO<sub>2</sub>, 92% air) on an orbital shaker  
 97 platform.

98 MARV (AFV31370.1), Angola (Q1PD50.1), Musoke (YP\_001531156.1), Ravn  
 99 (YP\_009055225.1), TAFV (Q66810), RESTV (Q66799), BOMV (YP\_009513277.1)  
 100 MLAV (YP\_010087186.1), LLOV (JF828358) GPs plasmid synthesized by  
 101 GENEWIZ and then cloned into the expression vector pcDNA3.1. EBOV  
 102 (A0A068J419), BDBV (AYI50382), SUDV (Q7T9D9) GPs and HIV-based vector  
 103 pSG3. Δenv. cmvFluc plasmids were kindly gifted by China Institute for Food and  
 104 Drug control.

### 105 Preparation of full-length antibody and antigen

106 AF-03 was selected from a human phage antibody library, which displays on the  
 107 surface of M13 bacteriophage particles. Screening procedures were as described in  
 108 detail previously<sup>34,35</sup>. Phage antibodies that bound to MARV GP protein were  
 109 obtained to express full-length IgGs using a standard protocol. In brief, the VH and

110 VL region of AF-03 were constructed into a mammalian full-length  
111 immunoglobulin expression vector pFRT-KIgG1 (Thermo, V601020), to generate  
112 plasmid AF-03. The human NPC2 gene (aa20-151) was linked to the VL of AF-03 by  
113 a short linker "TVAAP" and then constructed into pFRT-KIgG1 (designated as  
114 AF03-NL). The AF-03 and AF03-NL plasmid were transfected into ExpiCHO-S cells  
115 using the ExpiFectamine™ CHO Transfection Kit (Gibco, A29129) following the  
116 manufacturer's instructions. Purification was performed using ÄKTA prime plus  
117 system (GE Healthcare) with protein A column (GE Healthcare). MARV GP (Uganda  
118 strain) (aa 20-648, Δ277-455), CI-MPR1-3 (aa36-466) and NPC2 (aa20-151) gene  
119 with six-histidine-tagged at C-terminus was cloned into mammalian expression vector  
120 pcDNA3.1 and then transfected into HEK293T cells. MARV GP was purified using  
121 nickel column (GE Healthcare, 11003399). The concentration of proteins and  
122 antibodies were quantified by bicinchoninic acid (BCA) method.

## 123 ELISA

124 The 96-well enzyme-labelled array plates were coated with 2 µg/ml MARV-GP and  
125 mutated MARV GP (Q<sup>128</sup>S-N<sup>129</sup>S) respectively and incubated overnight at 4°C. Wells  
126 were washed for three times and blocked for 1 h at 37°C. A series of 12  
127 concentrations of AF-03 and MR78 were added and incubated for 1 h at 37 °C. Bound  
128 antibodies were detected with horseradish peroxidase (HRP)-labeled goat anti-human  
129 IgG secondary antibody (Invitrogen, A18817) at room temperature for 30 min.  
130 Binding signals were visualized using a TMB substrate (CWBIO, CW0050S) and the  
131 reaction was stopped by adding 2 N H<sub>2</sub>SO<sub>4</sub>. The light absorbance at 450 nm was

132 measured by microplate reader (Thermo Fisher Scientific). The concentration for 50%  
133 of maximal effect was defined as EC<sub>50</sub>.

134 For competitive ELISA, biotinylated AF-03 (1 µg/ml) was coated. MR78 and  
135 control mAb (Herceptin) in 3-fold serial dilution (ranging from 0.27 to 200 µg/ml)  
136 and added to the plates. After 1 h incubation at 37°C, the plates were washed and the  
137 bound Biotin-AF-03 was detected by adding horseradish peroxidase (HRP)-labeled  
138 Streptavidin (Thermo, S911). After a further 30 min incubation at room temperature,  
139 the plates were washed and TMB was added. The reaction was stopped by adding 2 N  
140 H<sub>2</sub>SO<sub>4</sub>. Absorbance was measured at 450 nm using a plate reader.

141 BLI analysis of antibody affinity

142 The binding affinity of AF-03 to MARV GP was measured by the Fortebio biofilm  
143 interferometry technique using anti-human IgG Fc capture (AHC) biosensors. In brief,  
144 8 µg/ml antibody was diluted to PBS containing 0.02% Tween 20 and immobilized in  
145 biosensors. The biosensors were then immersed with a serial dilutions of MARV GP  
146 to determine the association constant. Programs setting were following: baseline 60 s,  
147 loading 60 s, baseline 60 s, association 180 s, dissociation 220 s, regeneration 5 s.  
148 Baseline was performed with PBST buffer and regeneration was performed with 10  
149 mM glycine-HCl (pH 1.7) thrice. The data were analyzed using FortéBio Data  
150 Analysis 9.0 (Sartorius, FortéBio®).

151 Computer-guided homology modeling and molecular docking

152 The three-dimensional theoretical structure of fragment variable (FV) was constructed  
153 using computer-guided homology modeling approach based on the amino acid



154 sequences of the variable structural domains of the heavy and light chains of AF-03,  
155 and the conserved regions and loop structural domains were identified. The 3-D  
156 structure of the AF-03 Fv fragment was optimized under the consistent valence force  
157 field (CVFF) using the steepest descent and conjugate gradient minimization methods.  
158 The final minimized 3-D structure was evaluated by means of Ramachandran  
159 diagrams. In addition, the 3-D theoretical structure of the MARV GP protein was  
160 obtained and optimised using the CVFF force field. Under molecular docking method,  
161 the 3-D complex structures AF-03 Fv fragment and GP were obtained and optimized.  
162 With the determined 3-D structure of the AF-03 Fv fragment and GP, 50-ns molecular  
163 dynamics were performed with the Discovery\_3 module. All calculations were  
164 performed using Insight II 2000 software (MSI Co., San Diego) with IBM  
165 workstation.

#### 166 Pseudovirus preparation

167 HIVΔenvor (pSG3.Δenv.cmvFluc) bearing MARV, mutated MARV (Q<sup>128</sup>S-N<sup>129</sup>S,  
168 T<sup>204</sup>A-Q<sup>205</sup>A-T<sup>206</sup>A, Y<sup>218</sup>A, K<sup>222</sup>A and C<sup>226</sup>Y), EBOV (parental and 17 mutants  
169 indicated), SUDV, BDBV, TAFV, RESTV, BOMV, RAVN, MLAV and LLOV GPs  
170 were prepared by liposome-mediated transfection of HEK293T cells using JetPRIME  
171 (Polyplus Transfection, 25Y1801N5). Cells were seeded in 6-well plates at a density  
172 of 7×10<sup>5</sup> cells/well and transfected with 2 µg plasmids (0.4 µg GP and 1.6 µg  
173 HIVΔenvor) when cells reached 60-80% confluence. Supernatants were collected 48  
174 h after transfection, centrifuged to remove cell debris at 3,000 rpm for 10 min, filtered  
175 through a 0.45 µm-pore filter (Millipore, SLHUR33RB) and stored at -80°C.

176 Pseudovirus entry and antibody neutralization assay

177 Huh7 and HEK293T cells ( $3 \times 10^4$  cells/100  $\mu$ l/well) were infected with 100  $\mu$ l  
178 pseudovirus, which contained a luciferase reporter gene respectively. The luciferase  
179 activity were measured in a fluorescence microplate reader (Promega). The operation  
180 steps were following: after 36 h incubation at 37°C, 100  $\mu$ l of culture medium were  
181 discarded and addition with 100  $\mu$ l of Bright-Glo luciferase reagent (Promega, E6120)  
182 in each well. Mixtures were transfered to 96-well whiteboards after 2-minutes  
183 reaction to detect the relative luciferase intensity.

184 For AF-03 neutralization of MARV assays, 50  $\mu$ l mAb was 3-fold serially  
185 diluted and separately mixed with MARV pseudovirus at the same volume. The  
186 mixture were incubated at 37°C for 1 h, followed by the addition of 100  $\mu$ l cells  
187 ( $3 \times 10^4$  cells/well). 50% of maximal inhibitory concentration was defined as IC<sub>50</sub>. IC<sub>50</sub>  
188 values were determined by non-linear regression with least-squares fit in GraphPad  
189 Prism 8 (GraphPad Software).

190 In terms of AF-03 neutralization of ebola virus assays, pseudovirus (EBOV,  
191 SUDV and BDBV) were processed with thermolysin as previously described <sup>36</sup>.  
192 Briefly, Pseudotyped ebola virus were incubated at 37°C for 1 h with 200  $\mu$ g/ml  
193 thermolysin (Sigma, T7902). The reaction was stopped by addition of 400  $\mu$ M  
194 Phosphoramidon (Sigma, R7385) on ice for 20 min. The remaining steps followed  
195 AF-03 neutralization of MARV assays.

196 For AF03-NL neutralization assays, 50 l/well of serial diluted AF03-NL and  
197 AF-03 were incubated with cells at 37°C for 2 h to enable internalization of the

antibodies. 50 l/well of diluted pseudovirus was added to a 96-well plate and incubated at 37°C for 36 h. Bright-Glo luciferase reagent was added to detect the relative luciferase intensity.

#### Bioluminescent imaging in vivo

Four-week-old female BALB/c mice were purchased from Beijing Vital River Laboratory Animal Technology Co. Ltd. Mice were intraperitoneally injected with MARV pseudovirus (0.2 ml/mouse). AF-03 (10, 3 or 1 mg/kg) or control antibody Herceptin (10 mg/kg) were injected via intravenous route 24 h and 4 h before the pseudovirus injection respectively. Bioluminescent signals were monitored at Day 5. Briefly, D-luciferin (150 mg/kg body weight) (PerkinElmer, 122799) was intraperitoneally injected into the mice, and then exposed to Isoflurane alkyl for anesthesia. Bioluminescence was measured by the IVIS Lumina Series III Imaging System (Xenogen, Baltimore, MD, USA) with the living Image software. The signals emitted from different regions of the body were measured and presented as total fluxes. All data are presented as mean values  $\pm$  SEM.

#### Evaluation of internalization

HEK293T cells were counted  $3 \times 10^5$  cells, cold PBS washed twice and discarded the supernatant. 20 g/ml AF-03/AF03-NL was added and incubated at 4°C for 30 min. Then internalization group was transferred to 37°C for internalization for 30 min, while the control group continued to be incubated at 4°C for 30 min to adhere to the cell surface. The cells were washed with cold PBS, PE-anti-human IgG Fc secondary antibody (Biolegend, 41070) was added and incubated for 30 min at 4°C. The cells

220 were collected for analysis.

221 pHrodo Red labelling and immuno-localization

222 AF03-NL and AF-03 were covalently labeled with pH-sensitive pHrodo red

223 succinimidyl ester (Thermo, P36600) according to the manufacturer's instructions.

224 Antibodies were incubated with 10-fold molar excess of pHrodo red succinimidyl

225 ester for 1 h at room temperature. Excess unconjugated dye was removed using PD-10

226 desalting columns (GE Healthcare). pHrodo Red-labeled antibodies were exchanged

227 into HEPES buffer and concentrated in an Amicon Ultra centrifugal filter unit with a

228 nominal molecular weight cutoff of 30 kDa. Antibody concentration and degree of

229 labeling was determined according to the manufacturer's instructions.

230 HEK293T cells ( $1\sim2\times10^5$  cells per dish) were cultured overnight in confocal dish

231 pre-treated with polylysine (Beyotime, ST508) and then incubated with pHrodo

232 Red-labeled AF-03 and AF03-NL (20  $\mu\text{g/ml}$ ) at 37°C for 30 min. Unbound antibodies

233 were removed by washing with cold PBS. As well, cells were stained with cell

234 membrane dye (DiD) (Thermo, V22887) and Hoechst33342 (Thermo, H1398) at

235 37°C for 15 min. Single cells were analyzed for pHrodo Red fluorescence

236 on. Confocal Microscopy (dragonfly 200).

237 CI-MPR knockin and knockdown

238 Huh7 Cells were seeded in 6-well plates at  $3\times10^5$  cells/well and transfected with 2  $\mu\text{g}$

239 CI-MPR expression plasmids (JetPRIME) when cells reached 40-60% confluence and

240 cultured for 24 h. For CI-MPR silencing, HEK293T cells were seeded in 6-well plates

241 and transfected with siRNA-CI-MPR (Ribbio) and cultured for 48-72 h. CI-MPR

242 expression was detected by flow cytometry.

243 Flow cytometry

244 The cells were harvested and stained with FITC-conjugated anti-CI-MPR antibody

245 (Biolegend, 364207) on ice for 30 min. Cells were washed twice and detected on

246 FACS Aria II (BD Biosciences). Data analysis was performed using the FlowJo

247 software.

248 Statistical analyses

249 Data were analyzed, and the graphs were plotted using Prism software (GraphPad

250 Prism 8, San Diego, USA). The data are presented as the mean  $\pm$  standard error of the

251 mean. Intergroup differences were compared using unpaired t-tests or ANOVA. The *P*

252 <0.05 was considered statistically significant.

253

254

255

## 256 **Results**

### 257 **Characteristics of AF-03**

258 AF-03 was selected from a well-established phage surface display antibodies  
259 library with immense diversity in the selected complementarity determining region  
260 (CDR) loops<sup>34,35</sup>. We further subcloned VH and VL sequences of the antibody into a  
261 mammalian full-length immunoglobulin expression vector for full-length IgG  
262 expression. As shown in Fig. 1A, AF-03 was eukaryotically expressed with the purity  
263 over 95%. To determine the binding affinity, recombinant MARV GP without MLD  
264 was prepared (Fig. 1A). ELISA analysis showed that AF-03 bound to MARV GP with  
265 EC<sub>50</sub> of 0.16 µg/ml (Fig. 1B). Furthermore, BLI assay was done to determine the  
266 binding kinetics and showed that AF-03 bound to MARV GP with high affinity (K<sub>D</sub>  
267 value was less than 1x10<sup>-12</sup>M) (Fig. 1C). To identify determinants of MARV GP  
268 binding to AF-03, we utilized computer-guided homology modeling and molecular  
269 docking to generate computer models of MARV GP in complex with AF-03. Firstly,  
270 we obtained the theoretical 3-D structure of AF-03 Fv (Fig. 1D). Based on the 3-D  
271 structure of AF-03 and MARV GP separately, the 3-D complex structure of AF-03 and  
272 MARV GP achieved utilizing the molecular docking method, as shown in Fig. 1E.  
273 Overall, these data suggest the potency of AF-03 binding to MARV GP.

### 274 **Epitope mapping of MARV GP bound to AF-03**

275 Under CVFF forcefield, chosen steepest descent and conjugate gradient  
276 minimization methods, after 30,000 steps of minimization with the convergence  
277 criterion 0.02 kCal/mol, the optimized structure of the AF-03 Fv was evaluated. Using

a Ramachandran plot, the assignment of the whole heavy atoms of the AF-03 Fv was in the credible range. Through analyzing the van der Waals interactions, inter-molecular hydrogen bonds, polar interactions and electrostatic interactions between AF-03 and MARV GP, the key amino acid residues of MARV GP were selected for amino acid point mutations (Fig. 1F). T<sup>204</sup>-Q<sup>205</sup>-T<sup>206</sup>, Y<sup>218</sup> and K<sup>222</sup> were mutated to alanine, and Q<sup>128</sup>-N<sup>129</sup> were mutated to serine as well as C<sup>226</sup> was mutated to tyrosine. Firstly, We investigated if this mutated MARV species was still sensitive to AF-03 treatment. The inhibition assay revealed the impairment of neutralizing activity of AF-03 to mutated MARV pseudovirus, which indicates that Q<sup>128</sup>/N<sup>129</sup>/C<sup>226</sup> functions as key amino acids responsible for AF-03 neutralization (Fig. 2A left panel). To this end, we constructed the mutated MARV GP. ELISA assay showed that mutation of Q<sup>128</sup>S-N<sup>129</sup>S or C<sup>226</sup>Y significantly disrupted binding of GP to AF-03, while the binding and neutralizing capacity of MR78 to mutant GP and pseudovirus (C<sup>226</sup>Y), a mAb reported to be isolated from Marburg virus survivors<sup>16</sup>, was not almost affected (Fig. 2A right panel and B). Furthermore, we analyzed the secondary structure of the MARV GP and its mutants. By circular dichroism, the structure of both mutants was not obviously different from that of the parent GP (Fig. 3C, Tab. s1). Therefore, the weakened binding to the antibody was not due to the conformational change of the protein caused by the mutation. Competitive ELISA showed that AF-03 and MR78 could compete with each other to bind to MARV GP (Fig. 3D). These results indicate the epitopes of these two mAbs overlapped partially.

## 299 **In vitro neutralizing activity of AF-03**

Given the high binding affinity of AF-03 to MARV GP, we sought to determine whether AF-03 could impede MARV pseudotyped viral entry. An in vitro neutralization assay was developed based on full-length MARV GP-pseudotyped virus using a HIV $\Delta$ envor (pSG3. $\Delta$ env.cmvFluc). Liver and adrenal glands have been reported to be the early targets of MARV infection<sup>14,37</sup>. Therefore, we first tested the entry of MARV to hepatocyte cell line (Huh7) and HEK293T cells (renal cell line) by measuring the relative luciferase intensity. These two cell lines were susceptible to MARV cell entry. We used MR78 and cetuximab as positive and negative controls respectively. As expected, cetuximab had no effects on pseudotyped MARV entry. In contrast, AF-03 actively inhibited viral entry to HEK293T cells, with IC<sub>50</sub> value of 0.13  $\mu$ g/ml. As well, IC<sub>50</sub> of MR78 was 0.44  $\mu$ g/ml (Fig. 3A left panel). In Huh7 cells, IC<sub>50</sub> of AF-03 and MR78 was 0.4 and 1.03  $\mu$ g/ml, respectively (Fig. 3A right panel). These results suggest that AF-03 had more potency of neutralization than MR78. We also conducted AF-03 neutralization experiments on pseudotyped Angola, Musoke and Ravn strains and showed strong and comparable neutralizing ability to all these strains (IC<sub>50</sub> was 0.32, 0.12 and 0.15  $\mu$ g/ml respectively) (Fig. 3B). Taken together, these data suggest that AF-03 harbors prominent neutralizing activity to MARV infection.

### **In vivo preventive efficacy of AF-03**

To verify the in vivo preventive efficacy, AF-03 was intravenously injected into mice before pseudotyped MARV exposure (-24 h and -4 h) respectively. The bioluminescence intensity was measured on day 5 after pseudovirus injection. As



322 shown in Fig. 3C and D, AF-03-treated group displayed  
323 lower bioluminescence activity compared with the control group, while the treatment  
324 with control antibodies had no effects. Administration of 1 mg/kg AF-03 prior to the  
325 injection of MARV could decrease viral infection to approximately 50% level and  
326 increasing doses of AF-03 led to higher preventive efficacy. This indicates clearly that  
327 AF-03 is capable of preventing against MARV infection in a dose-dependent manner  
328 and represents a potential candidate for MARV prophylaxis.

### 329 **AF-03 impedes cell entry of EBOV, SUDV and BDBV harboring GPcl**

330 Given the close structural similarity of Marburg virus to ebola virus, to  
331 determine whether AF-03 was also available to the treatment of EBOV infection, we  
332 conducted neutralization of pseudotyped EBOV, SUDV and BDBV with AF-03. In  
333 addition, considering that glycan cap or mucin-like domain are known to mask the  
334 putative receptor-binding domain on EBOV, SUDV and BDBV GP, leading to  
335 blockade of engagement between AF-03 and GP<sup>16</sup>. Furthermore, in vitro cleavage of  
336 particles with thermolysin functionally mimics the cleavage due to the combination of  
337 cathepsin L and cathepsin B. Accordingly, glycan cap and mucin-like domain were  
338 enzymatically cleaved by digesting GP with 250 µg/ml thermolysin at 37°C.  
339 Consequently, the inhibitory function of AF-03 on cell entry of all three species of  
340 ebola virus bearing cleaved GP was much stronger than those bearing uncleaved GP  
341 (Fig. 4). Overall, these data suggest that AF-03 has therapeutic potentials for EBOV,  
342 SUDV and BDBV infection.

### 343 **The potency of NPC2-fused AF-03 to be delivered into the endosome**

344 Given the inability of AF-03 to transport into endosomal compartment where intact  
345 GP is cleaved by cathepsin B/L, we engaged NPC2 to the N-terminus of light chain of  
346 AF-03 (Fig. s1A), according to a protocol described previously<sup>38</sup>. As well, we  
347 produced the 1-3 domain of CI-MPR (Fig. s1A), which is a ligand for NPC2 and  
348 expressed on the cellular and endosomal membrane<sup>32</sup>. The results showed that  
349 NPC2-fused AF-03 (termed AF03-NL), rather than AF-03, bound to CI-MPR1-3 (Fig.  
350 s1B). Next we investigated the internalization of AF03-NL. AF03-NL or AF-03 was  
351 incubated with HEK293T cells, which expressed CI-MPR (Fig. s2A), at 4°C for  
352 attachment. As expected, AF03-NL instead of AF-03 adhered to the cell surface,  
353 detected by fluorescence-labelled secondary IgG. Upon endocytosis, the fluorescence  
354 on the cell surface decreased dramatically, implying the occurrence of AF03-NL  
355 internalization (Fig. 5A). To further address this issue, AF-03 and AF03-NL were  
356 labelled by pHrodo Red dye that is sensitive to acidic niche. Accord with Fig. 5A,  
357 pHrodo Red-conjugated AF03-NL was observed in the acidic endosomal  
358 compartment by flow cytometry and fluorescence microscopy respectively (Fig. 5B  
359 and C). In contrast, AF-03 was not seen in the endosome.

### 360 **Pan-filovirus inhibition of cell entry by AF03-NL via engagement between NPC2** 361 **and CI-MPR**

362 We first compared the binding of AF03-NL/AF-03 to MARV GP. ELISA showed  
363 relatively weak binding activity of AF03-NL compared with AF-03 (Fig. s3A). We  
364 thereafter evaluated the neutralizing activity of AF03-NL to MARV pseudovirus.  
365 Intriguingly, AF03-NL showed stronger neutralizing activity than AF-03 (The IC<sub>50</sub>

366 was 0.057 and 0.284 g/ml, respectively) (Fig. s3B), which may be attributed to  
 367 sustained tethering of AF03-NL to pseudovirus at extracellular space as well as  
 368 endosomal compartment. Next we compared the neutralizing activity of AF03-NL and  
 369 AF-03 to a series of filovirus species. AF03-NL displayed superior neutralizing  
 370 activity to other nine filovirus species. While, no or weak inhibition of entry by AF-03  
 371 was found (Fig. 6A). Furthermore, AF03-NL, instead of AF-03, also actively inhibited  
 372 cell entry of 17 EBOV mutants that were detected in natural hosts (Fig. 6B).

373 To investigate the mechanisms mediating the potency of AF03-NL, we produced  
 374 NPC2 protein (Fig.7A) and then examined the inhibition of EBOV entry by AF03-NL  
 375 or the mixture of AF-03 and NPC2. AF-03, NPC2 alone or in combination did not  
 376 inhibit EBOV entry. Conversely, AF03-NL actively impeded this process (Fig. 7B).  
 377 To clarify whether this effect is CI-MPR-dependent, CI-MPR in HEK293T cells was  
 378 silenced (Fig. 7C). The result showed that CI-MPR knockdown rendered significant  
 379 abrogation of the inhibitory ability of AF03-NL (Fig. 7C). We also introduced  
 380 CI-MPR into Huh7 cell line that is null for this receptor (Fig. s2B). The inhibitory  
 381 effects of AF03-NL were augmented in CI-MPR-overexpressed cells compared with  
 382 empty vector-introduced counterparts (Fig. 7D). Taken together, these data indicate  
 383 that the inhibitory potency of AF03-NL is dependent on the interaction between NPC2  
 384 and CI-MPR.

385

## 386 Discussion

387 The Marburg virus was initially identified after simultaneous outbreaks in  
 388 Marburg and Frankfurt in Germany in 1967<sup>16,39</sup>. To date, there have been a dozen  
 389 outbreaks of Marburg virus infection in humans<sup>40</sup>. Giving the recurrence of  
 390 Marburg virus outbreaks and its high virulence and lethality, there is an urgent need to  
 391 develop prophylactic and therapeutic interventions for Marburg infections. MARV  
 392 GP is a surface viral protein, which is responsible for host receptor binding and cell  
 393 entry thus provides an attractive target for the development of antagonists. Flyak et al.  
 394 screened several MARV GP-specific neutralizing antibodies from the plasma of a  
 395 MARV-infected survivor, which achieved 100% protection in mice subjected to  
 396 mouse-adapted MARV challenge<sup>41</sup>. The MARV GP-specific antibody cocktail was  
 397 also developed, 3 mAbs cocktail could protect hamster from lethal hamster-adapted  
 398 MARV infection, while treatment with either one or two antibodies failed<sup>42</sup>.

399 In this study, we selected an antibody from a human antibody phage library and  
 400 the affinity constant reached the  $1 \times 10^{-12}$ M level. The neutralizing activities of the  
 401 antibody were demonstrated by utilizing pseudotyped MARV Uganda strain. The  
 402 results showed that AF-03 effectively inhibits HIV $\Delta$ envor (pSG3. $\Delta$ env.cmvFluc)  
 403 pseudotyped MARV viral entry at IC<sub>50</sub> of 0.13 and 0.4  $\mu$ g/ml in HEK293T and Huh7  
 404 respectively. Furthermore, compared with control antibody, AF-03 exhibited a  
 405 protective property against pseudovirus infection in mice. Epitope mapping results  
 406 showed that GP Q<sup>128</sup>-N<sup>129</sup> and C<sup>226</sup> was the binding and functional epitope that  
 407 interacted with AF-03, which means AF-03 targeting the interface of GP-NPC1

408 interaction, considering that N129 is known to be located in the NPC1 binding  
409 domain. RBDs are highly conserved among filovirus species, so they are an attractive  
410 target for broadly effective anti-filovirus drug development<sup>49</sup>. We found that AF-03  
411 also bound to EBOV GPcl and can neutralized ebola viruses bearing in vitro cleaved  
412 GP, suggesting that AF-03 represents a good candidate for endosome-delivering  
413 strategy by ligation to another mAb against a surface-exposed EBOV GP epitope or a  
414 ligand peptide for host cation-independent mannose-6-phosphate receptor<sup>38</sup>, which  
415 will ultimately affords cross-reactivity against multiple filovirus species. Accordingly,  
416 we designed NPC2-fused AF-03 and demonstrated its broad-spectrum inhibitory  
417 capacity to filovirus species and EBOV mutants. Future investigations on the  
418 inhibition of AF03-NL to authentic virus infection in vitro and in vivo are warranted.

419 Overall, our study identified a high-affinity anti-MARV antibody AF-03  
420 targeting a conserved and hidden site at the filovirus GPcl-NPC1 interface, which was  
421 capable of neutralizing MARV infection both in vitro and in vivo. Furthermore,  
422 AF-03 may be a potential candidate for the effective protection against pan-filovirus  
423 species infection. Investigations on AF-03 treatment of mice challenged by authentic  
424 virus are undergoing.

425

## 426     **Abbreviations**

427            MARV: Marburg virus; EBOV: Ebola virus; SUDV: Sudan virus; BDBV:

428     Bundibugy virus; mAb: monoclonal antibody; PBS: phosphate-buffered saline; GP:

429     glycoprotein; RAVN: Ravn virus; RESTV: Reston virus; TAFV: Tai forest virus;

430     MVD: Marburg virus disease; EVD: EBOV virus; RBD: receptor binding domain;

431     MLD: mucin like domain; NPC1: Niemann-Pick C1; CDR: complementarity

432     determining region; CVFF: consistent valence force field; FV: fragment variable;

433     CI-MPR: cation-independent mannose-6-phosphate receptor; NPC2: Niemann-Pick

434     C2

435

436

437 **Compliance with ethics guidelines**

438 Yuting Zhang, Min Zhang, Haiyan Wu, Xinwei Wang, Hang Zheng, Junjuan Feng,

439 Jing Wang, Longlong Luo, He Xiao, Chunxia Qiao, Xinying Li, Yuanqiang Zheng,

440 Weijin Huang, Youchun Wang, Yi Wang, Yanchun Shi, Jiannan Feng, Guojiang Chen

441 declare that they have no competing interests.

442

443

#### 444 **Author contributions**

445 Guojiang Chen, Jiannan Feng, Yanchun Shi and Yi Wang conceived and designed  
 446 this study. Guojiang Chen, Jiannan Feng and Yuanqiang Zheng provided funding  
 447 support. Yuting Zhang, Min Zhang, Haiyan Wu and Xinwei Wang performed of the  
 448 experiments and prepared the manuscript. Hang Zheng and Junjuan Feng were  
 449 involved in optimization of the experimental protocols. Jing Wang, Longlong Luo, He  
 450 Xiao, Chunxia Qiao, Xinying Li, Yuanqiang Zheng, Weijin Huang, Youchun Wang  
 451 provided methodological support. All authors contributed to the article and approved  
 452 the submitted version.

453

454



455    **Acknowledgments**

456    This work is granted from the National Natural Science Foundation of China  
457    (81672803, 31771010, 81871252).

458

459

460    **Ethics approval**

461    The animal study was reviewed and approved by the Institutional Animal Care and  
462    Use Committee of Academy of Military Medical Sciences.

463

464

## 465      **References**

- 466      1.Amarasinghe, G.K., Aylón, M.A., Bào, Y., Basler, C.F., Bavari, S., Blasdel, K.R., Bries, T., Brown, P.A.,  
467      Bukreyev, A., Balkema-Buschmann, A., et al. (2019). Taxonomy of the order Mononegavirales: update  
468      2019. *Arch Virol* 164, 1967-1980. 10.1007/s00705-019-04247-4.
- 469      2.Baseler, L., Chertow, D.S., Johnson, K.M., Feldmann, H., and Morens, D.M. (2017). The Pathogenesis  
470      of Ebola Virus Disease. *Annu Rev Pathol* 12, 387-418. 10.1146/annurev-pathol-052016-100506.
- 471      3.Kuhn, J.H., Adachi, T., Adhikari, N.K.J., Arribas, J.R., Bah, I.E., Bausch, D.G., Bhadelia, N., Borchert, M.,  
472      Brantsæter, A.B., Brett-Major, D.M., et al. (2019). New filovirus disease classification and  
473      nomenclature. *Nat Rev Microbiol* 17, 261-263. 10.1038/s41579-019-0187-4.
- 474      4.Bào, Y., Amarasinghe, G.K., Basler, C.F., Bavari, S., Bukreyev, A., Chandran, K., Dolnik, O., Dye, J.M.,  
475      Ebihara, H., Formenty, P., et al. (2017). Implementation of Objective PASC-Derived Taxon Demarcation  
476      Criteria for Official Classification of Filoviruses. *Viruses* 9. 10.3390/v9050106.
- 477      5.Ristanović, E.S., Kokoškov, N.S., Crozier, I., Kuhn, J.H., and Gligić, A.S. (2020). A Forgotten Episode of  
478      Marburg Virus Disease: Belgrade, Yugoslavia, 1967. *Microbiol Mol Biol Rev* 84.  
479      10.1128/MMBR.00095-19.
- 480      6.Fan, P., Chi, X., Liu, G., Zhang, G., Chen, Z., Liu, Y., Fang, T., Li, J., Banadyga, L., He, S., et al. (2020).  
481      Potent neutralizing monoclonal antibodies against Ebola virus isolated from vaccinated donors. *mAbs*  
482      12, 1742457. 10.1080/19420862.2020.1742457.
- 483      7.Goldstein, T., Anthony, S.J., Gbakima, A., Bird, B.H., Bangura, J., Tremeau-Bravard, A., Belaganahalli,  
484      M.N., Wells, H.L., Dhanota, J.K., Liang, E., et al. (2018). The discovery of Bombali virus adds further  
485      support for bats as hosts of ebolaviruses. *Nat Microbiol* 3, 1084-1089. 10.1038/s41564-018-0227-2.
- 486      8.Negredo, A., Palacios, G., Vázquez-Morón, S., González, F., Dopazo, H., Molero, F., Juste, J., Quetglas,  
487      J., Savji, N., de la Cruz Martínez, M., et al. (2011). Discovery of an ebolavirus-like filovirus in europe.  
488      *PLoS Pathog* 7, e1002304. 10.1371/journal.ppat.1002304.
- 489      9.Kemenesi, G., Tóth, G.E., Mayora-Neto, M., Scott, S., Temperton, N., Wright, E., Mühlberger, E.,  
490      Hume, A.J., Suder, E.L., Zana, B., et al. (2022). Isolation of infectious Lloviu virus from Schreiber's bats  
491      in Hungary. *Nat Commun* 13, 1706. 10.1038/s41467-022-29298-1.
- 492      10.Yang, X.L., Tan, C.W., Anderson, D.E., Jiang, R.D., Li, B., Zhang, W., Zhu, Y., Lim, X.F., Zhou, P., Liu, X.L.,  
493      et al. (2019). Characterization of a filovirus (Měnglà virus) from Rousettus bats in China. *Nat Microbiol*  
494      4, 390-395. 10.1038/s41564-018-0328-y.
- 495      11.Mehedi, M., Groseth, A., Feldmann, H., and Ebihara, H. (2011). Clinical aspects of Marburg  
496      hemorrhagic fever. *Future Virol* 6, 1091-1106. 10.2217/fvl.11.79.
- 497      12.Beniach, D.R., and Booth, T.F. (2017). Structure of the Ebola virus glycoprotein spike within the virion  
498      envelope at 11 Å resolution. *Sci Rep* 7, 46374. 10.1038/srep46374.
- 499      13.Lee, J.E., and Saphire, E.O. (2009). Neutralizing ebolavirus: structural insights into the envelope  
500      glycoprotein and antibodies targeted against it. *Curr Opin Struct Biol* 19, 408-417.  
501      10.1016/j.sbi.2009.05.004.
- 502      14.Brauburger, K., Hume, A.J., Mühlberger, E., and Olejnik, J. (2012). Forty-five years of Marburg virus  
503      research. *Viruses* 4, 1878-1927. 10.3390/v4101878.
- 504      15.Schafer, A., Xiong, R., Cooper, L., Nowar, R., Lee, H., Li, Y., Ramirez, B.E., Peet, N.P., Caffrey, M.,  
505      Thatcher, G.R.J., et al. (2021). Evidence for distinct mechanisms of small molecule inhibitors of filovirus  
506      entry. *PLoS Pathog* 17, e1009312. 10.1371/journal.ppat.1009312.
- 507      16.Hashiguchi, T., Fusco, M.L., Bornholdt, Z.A., Lee, J.E., Flyak, A.I., Matsuoka, R., Kohda, D., Yanagi, Y.,

508 Hammel, M., Jr, J.E.C., and Saphire, E.O. (2015). Structural basis for Marburg virus neutralization by a  
509 cross-reactive human antibody. *Cell* 160, 904-912. 10.1016/j.cell.2015.01.041.

510 17.Fusco, M.L., Hashiguchi, T., Cassan, R., Biggins, J.E., Murin, C.D., Warfield, K.L., Li, S., Holtsberg, F.W.,  
511 Shulenin, S., Vu, H., et al. (2015). Protective mAbs and Cross-Reactive mAbs Raised by Immunization  
512 with Engineered Marburg Virus GPs. *PLoS Pathog* 11, e1005016. 10.1371/journal.ppat.1005016.

513 18.Gregory, S.M., Harada, E., Liang, B., Delos, S.E., White, J.M., and Tamm, L.K. (2011). Structure and  
514 function of the complete internal fusion loop from Ebolavirus glycoprotein 2. *Proc Natl Acad Sci U S A*  
515 108, 11211-11216. 10.1073/pnas.1104760108.

516 19.Lee, J., Nyenhuis, D.A., Nelson, E.A., Cafiso, D.S., White, J.M., and Tamm, L.K. (2017). Structure of  
517 the Ebola virus envelope protein MPER/TM domain and its interaction with the fusion loop explains  
518 their fusion activity. *Proc Natl Acad Sci U S A* 114, E7987-E7996. 10.1073/pnas.1708052114.

519 20.Volchkov, V.E., Volchkova, V.A., Ströher, U., Becker, S., Dolnik, O., Cieplik, M., Garten, W., Klenk, H.D.,  
520 and Feldmann, H. (2000). Proteolytic processing of Marburg virus glycoprotein. *Virology* 268, 1-6.  
521 10.1006/viro.1999.0110.

522 21.Dye, J.M., Herbert, A.S., Kuehne, A.I., Barth, J.F., Muhammad, M.A., Zak, S.E., Ortiz, R.A., Prugar, L.I.,  
523 and Pratt, W.D. (2012). Postexposure antibody prophylaxis protects nonhuman primates from filovirus  
524 disease. *Proc Natl Acad Sci U S A* 109, 5034-5039. 10.1073/pnas.1200409109.

525 22.Aleksandrowicz, P., Marzi, A., Biedenkopf, N., Beimforde, N., Becker, S., Hoenen, T., Feldmann, H.,  
526 and Schnittler, H.-J. (2011). Ebola virus enters host cells by macropinocytosis and clathrin-mediated  
527 endocytosis. *J Infect Dis* 204 Suppl 3, S957-967. 10.1093/infdis/jir326.

528 23.Saeed, M.F., Kolokoltsov, A.A., Albrecht, T., and Davey, R.A. (2010). Cellular entry of ebola virus  
529 involves uptake by a macropinocytosis-like mechanism and subsequent trafficking through early and  
530 late endosomes. *PLoS Pathog* 6, e1001110. 10.1371/journal.ppat.1001110.

531 24.Carette, J.E., Raaben, M., Wong, A.C., Herbert, A.S., Obernosterer, G., Mulherkar, N., Kuehne, A.I.,  
532 Kranzusch, P.J., Griffin, A.M., Ruthel, G., et al. (2011). Ebola virus entry requires the cholesterol  
533 transporter Niemann-Pick C1. *Nature* 477, 340-343. 10.1038/nature10348.

534 25.Brecher, M., Schornberg, K.L., Delos, S.E., Fusco, M.L., Saphire, E.O., and White, J.M. (2012).  
535 Cathepsin cleavage potentiates the Ebola virus glycoprotein to undergo a subsequent fusion-relevant  
536 conformational change. *J Virol* 86, 364-372. 10.1128/JVI.05708-11.

537 26.Martinez, O., Johnson, J., Manicassamy, B., Rong, L., Olinger, G.G., Hensley, L.E., and Basler, C.F.  
538 (2010). Zaire Ebola virus entry into human dendritic cells is insensitive to cathepsin L inhibition.  
539 *Cellular Microbiology* 12, 148-157. 10.1111/j.1462-5822.2009.01385.x.

540 27.Gnirss, K., Kühl, A., Karsten, C., Glowacka, I., Bertram, S., Kaup, F., Hofmann, H., and Pöhlmann, S.  
541 (2012). Cathepsins B and L activate Ebola but not Marburg virus glycoproteins for efficient entry into  
542 cell lines and macrophages independent of TMPRSS2 expression. *Virology* 424, 3-10.  
543 10.1016/j.virol.2011.11.031.

544 28.Misasi, J., Chandran, K., Yang, J.-Y., Considine, B., Filone, C.M., Côté, M., Sullivan, N., Fabozzi, G.,  
545 Hensley, L., and Cunningham, J. (2012). Filoviruses require endosomal cysteine proteases for entry but  
546 exhibit distinct protease preferences. *J Virol* 86, 3284-3292. 10.1128/JVI.06346-11.

547 29.Hu, N., Qiao, C., Wang, J., Wang, Z., Li, X., Zhou, L., Wu, J., Zhang, D., Feng, J., Shen, B., et al. (2021).  
548 Identification of a novel protective human monoclonal antibody, LX8, that targets the key  
549 neutralizing epitopes of staphylococcal enterotoxin B. *Biochem Biophys Res Commun* 549, 120-127.  
550 10.1016/j.bbrc.2021.02.057.

551 30.Wang, Z., Hu, N., Zhou, Y., Shi, N., Shen, B., Luo, L., and Feng, J. (2022). Structure-guided affinity

552 maturation of a novel human antibody targeting the SARS-CoV-2 nucleocapsid protein. *Scientific*  
553 *Reports* **12**, 8469. 10.1038/s41598-022-12242-0.

554 31.Dahms, N.M., Olson, L.J., and Kim, J.J. (2008). Strategies for carbohydrate recognition by the  
555 mannose 6-phosphate receptors. *Glycobiology* **18**, 664-678. 10.1093/glycob/cwn061.

556 32.Bohnsack, R.N., Song, X., Olson, L.J., Kudo, M., Gotschall, R.R., Canfield, W.M., Cummings, R.D.,  
557 Smith, D.F., and Dahms, N.M. (2009). Cation-independent mannose 6-phosphate receptor: a  
558 composite of distinct phosphomannosyl binding sites. *J Biol Chem* **284**, 35215-35226.  
559 10.1074/jbc.M109.056184.

560 33.Grubb, J.H., Vogler, C., and Sly, W.S. (2010). New strategies for enzyme replacement therapy for  
561 lysosomal storage diseases. *Rejuvenation Res* **13**, 229-236. 10.1089/rej.2009.0920.

562 34.Duan, Y., Luo, L., Qiao, C., Li, X., Wang, J., Liu, H., Zhou, T., Shen, B., Lv, M., and Feng, J. (2019). A  
563 novel human anti-AXL monoclonal antibody attenuates tumour cell migration. *Scandinavian journal of*  
564 *immunology*. 10.1111/sji.1277.

565 35.Liu, F., Guan, Z., Liu, Y., Li, J., Liu, C., Gao, Y., Ma, Y., Feng, J., Shen, B., and Yang, G. (2021).  
566 Identification of a Human Anti-Alpha-Toxin Monoclonal Antibody Against *Staphylococcus aureus*  
567 Infection. *Frontiers in Microbiology* **12**, 1875-. 10.3389/fmicb.2021.692279.

568 36.Markosyan, R.M., Miao, C., Zheng, Y.-M., Melikyan, G.B., Liu, S.-L., and Cohen, F.S. (2016). Induction  
569 of Cell-Cell Fusion by Ebola Virus Glycoprotein: Low pH Is Not a Trigger. *PLoS Pathog* **12**, e1005373.  
570 10.1371/journal.ppat.1005373.

571 37.Shifflett, K., and Marzi, A. (2019). Marburg virus pathogenesis - differences and similarities in  
572 humans and animal models. *Virology* **16**, 165. 10.1186/s12985-019-1272-z.

573 38.Wirchnianski, A.S., Wec, A.Z., Nyakatura, E.K., Herbert, A.S., Slough, M.M., Kuehne, A.I., Mittler, E.,  
574 Jangra, R.K., Teruya, J., Dye, J.M., et al. (2021). Two Distinct Lysosomal Targeting Strategies Afford  
575 Trojan Horse Antibodies With Pan-Filovirus Activity. *Frontiers in immunology* **12**, 729851.  
576 10.3389/fimmu.2021.729851.

577 39.Abir, M.H., Rahman, T., Das, A., Etu, S.N., Nafiz, I.H., Rakib, A., Mitra, S., Emran, T.B., Dhama, K.,  
578 Islam, A., et al. (2022). Pathogenicity and virulence of Marburg virus. *Virulence* **13**, 609-633.  
579 10.1080/21505594.2022.2054760.

580 40.Araf, Y., Maliha, S.T., Zhai, J., and Zheng, C. (2023). Marburg virus outbreak in 2022: a public health  
581 concern. *Lancet Microbe* **4**, e9. 10.1016/s2666-5247(22)00258-0.

582 41.Flyak, A.I., Ilinykh, P.A., Murin, C.D., Garron, T., Shen, X., Fusco, M.L., Hashiguchi, T., Bornholdt, Z.A.,  
583 Slaughter, J.C., Sapparapu, G., et al. (2015). Mechanism of human antibody-mediated neutralization of  
584 Marburg virus. *Cell* **160**, 893-903. 10.1016/j.cell.2015.01.031.

585 42.Marzi, A., Haddock, E., Kajihara, M., Feldmann, H., and Takada, A. (2018). Monoclonal Antibody  
586 Cocktail Protects Hamsters From Lethal Marburg Virus Infection. *J Infect Dis* **218**, S662-S665.  
587 10.1093/infdis/jiy235.

588 43.Kan, S.H., Troitskaya, L.A., Sinow, C.S., Haitz, K., Todd, A.K., Di Stefano, A., Le, S.Q., Dickson, P.I., and  
589 Tippin, B.L. (2014). Insulin-like growth factor II peptide fusion enables uptake and lysosomal delivery  
590 of  $\alpha$ -N-acetylglucosaminidase to mucopolysaccharidosis type IIIB fibroblasts. *Biochem J* **458**, 281-289.  
591 10.1042/bj20130845.

592 44.Aoyagi-Scharber, M., Crippen-Harmon, D., Lawrence, R., Vincelette, J., Yogalingam, G., Prill, H., Yip,  
593 B.K., Baridon, B., Vitelli, C., Lee, A., et al. (2017). Clearance of Heparan Sulfate and Attenuation of CNS  
594 Pathology by Intracerebroventricular BMN 250 in Sanfilippo Type B Mice. *Mol Ther Methods Clin Dev*

595 6, 43-53. 10.1016/j.omtm.2017.05.009.  
596 45.Kan, S.H., Aoyagi-Scharber, M., Le, S.Q., Vincelette, J., Ohmi, K., Bullens, S., Wendt, D.J.,  
597 Christianson, T.M., Tiger, P.M., Brown, J.R., et al. (2014). Delivery of an enzyme-IGFII fusion protein to  
598 the mouse brain is therapeutic for mucopolysaccharidosis type IIIB. *Proc Natl Acad Sci U S A* *111*,  
599 14870-14875. 10.1073/pnas.1416660111.  
600 46.Berthe, M.L., Esslimani Sahla, M., Roger, P., Gleizes, M., Lemamy, G.J., Brouillet, J.P., and Rochefort,  
601 H. (2003). Mannose-6-phosphate/insulin-like growth factor-II receptor expression levels during the  
602 progression from normal human mammary tissue to invasive breast carcinomas. *Eur J Cancer* *39*,  
603 635-642. 10.1016/s0959-8049(02)00627-5.  
604 47.Jonson, T., Albrechtsson, E., Axelson, J., Heidenblad, M., Gorunova, L., Johansson, B., and Höglund,  
605 M. (2001). Altered expression of TGFB receptors and mitogenic effects of TGFB in pancreatic  
606 carcinomas. *Int J Oncol* *19*, 71-81.  
607 48.Pavelić, K., Kolak, T., Kapitanović, S., Radošević, S., Spaventi, S., Kruslin, B., and Pavelić, J. (2003).  
608 Gastric cancer: the role of insulin-like growth factor 2 (IGF 2) and its receptors (IGF 1R and M6-P/IGF  
609 2R). *J Pathol* *201*, 430-438. 10.1002/path.1465.  
610 49.Densumite, J., Phanthong, S., Seesuy, W., Sookrung, N., Chaisri, U., and Chaicumpa, W. (2021).  
611 Engineered Human Monoclonal scFv to Receptor Binding Domain of Ebolavirus. *Vaccines* *9*.  
612 10.3390/vaccines9050457.

613

614

## 615 **Figure legends**

### 616 **Figure 1. Binding activity of mAb AF-03 to MARV GP and its epitopes.**

617 (A) AF-03 and MARV GP proteins are examined by SDS-PAGE. NR, non-reducing;  
 618 R, reducing. (B) The binding activity of AF-03 to MARV GP is determined by ELISA.  
 619 The absorbance is detected at 450 nm. (C) The binding kinetics of AF-03 to MARV  
 620 GP is detected by BLI with a 180-s association step followed by a 220-s dissociation  
 621 step. Experiments are independently repeated at least three times, and the data from  
 622 one representative experiment is shown. (D) The 3-D ribbon structures of the AF-03  
 623 Fv fragment. The red ribbon denotes H-CDR1, the light blue denotes H-CDR2, the  
 624 pink denotes H-CDR3, the orange denotes L-CDR1, the deep blue denotes L-CDR2,  
 625 the purple denotes L-CDR3. (E) AF-03 and MARV GP complex derived from  
 626 theoretical modeling. The green ribbon denotes the orientation of the MARV GP  
 627 fragment, the yellow denotes AF-03 VLCDR, the pink denotes AF-03 VHCDR, the  
 628 deep blue denotes AF-03 VL and the red ribbon denotes AF-03 VH. (F) By molecular  
 629 docking analysis of van der Waals interaction, intermolecular hydrogen bonding,  
 630 polarity interaction and electrostatic interaction, the key amino acid residues of  
 631 MARV GP are screened.

632

### 633 **Figure 2. AF-03 Epitope Identification.**

634 (A) The neutralization activity of AF-03 or MR78 to mutated pseudovirus  
 635 ( $Q^{128}S-N^{129}S$ ,  $Q^{204}A-T^{205}A-Q^{206}A$ ,  $Y^{218}A$ ,  $K^{222}A$ ,  $C^{226}Y$ ) is evaluated in HEK293T  
 636 cells. The inhibition rate is analyzed. (B) The binding of AF-03 and MR78 to mutant

GP ( $Q^{128}S-N^{129}S$  or  $C^{226}Y$ ) is examined by ELISA respectively. (C) Secondary structure of mutants and MARV GP is detected by CD. (D) The epitope overlapping between AF-03 and MR78 is examined by the competition ELISA.

**Figure 3. In vitro and in vivo neutralization of MARV pseudovirus infection by AF-03.**

(A) Pseudotypic MARV-Uganda is incubated with AF-03, MR78 or control mAb at 37°C for 1 h before infecting HEK293T cells (left) and Huh7 cells (right) respectively. Luciferase is assayed and inhibition rates are calculated. (B) Pseudotypic MARV-Angola, Musoke and Ravn infect HEK293T cells respectively and neutralization activity of AF-03 to these species is determined. (C) AF-03 (10, 3, 1mg/kg) is administrated at 24 and 4 h before intraperitoneal injection of pseudovirus. On day 5, bioluminescence signals are detected by an IVIS Lumina Series III imaging system. (D) The average radiance value based on the luminescence of (C),  $*p<0.05$ ,  $**p<0.01$ ,  $***p<0.001$ .

**Figure 4. The neutralization activity of AF-03 to EBOV, SUDV and BDBV harboring cleaved GP.**

Pseudotypic EBOV, SUDV, and BDBV are processed with thermolysin at 37°C. Inhibition of these ebola virus infection harboring GP or GPcl by AF-03 is examined by luciferase assay.  $*p<0.05$ ,  $**p<0.01$ ,  $***p<0.001$



**Figure 5. Cellular internalization of AF03-NL.**

(A) AF-03 or AF03-NL is incubated with cells at 4°C for 1h to prevent internalization and then at 37°C for another 2 h to allow internalization. PE-conjugated secondary antibody is added prior to analysis by flow cytometry. (B,C) pHrodo Red-labelled AF-03 or AF03-NL is incubated with cells at 37°C for 1h and analyzed by flow cytometry (B) and fluorescence microscopy (C) respectively. The red arrow denotes internalized AF03-NL. Experiments are independently repeated at least three times, and the data from one representative experiment is shown.

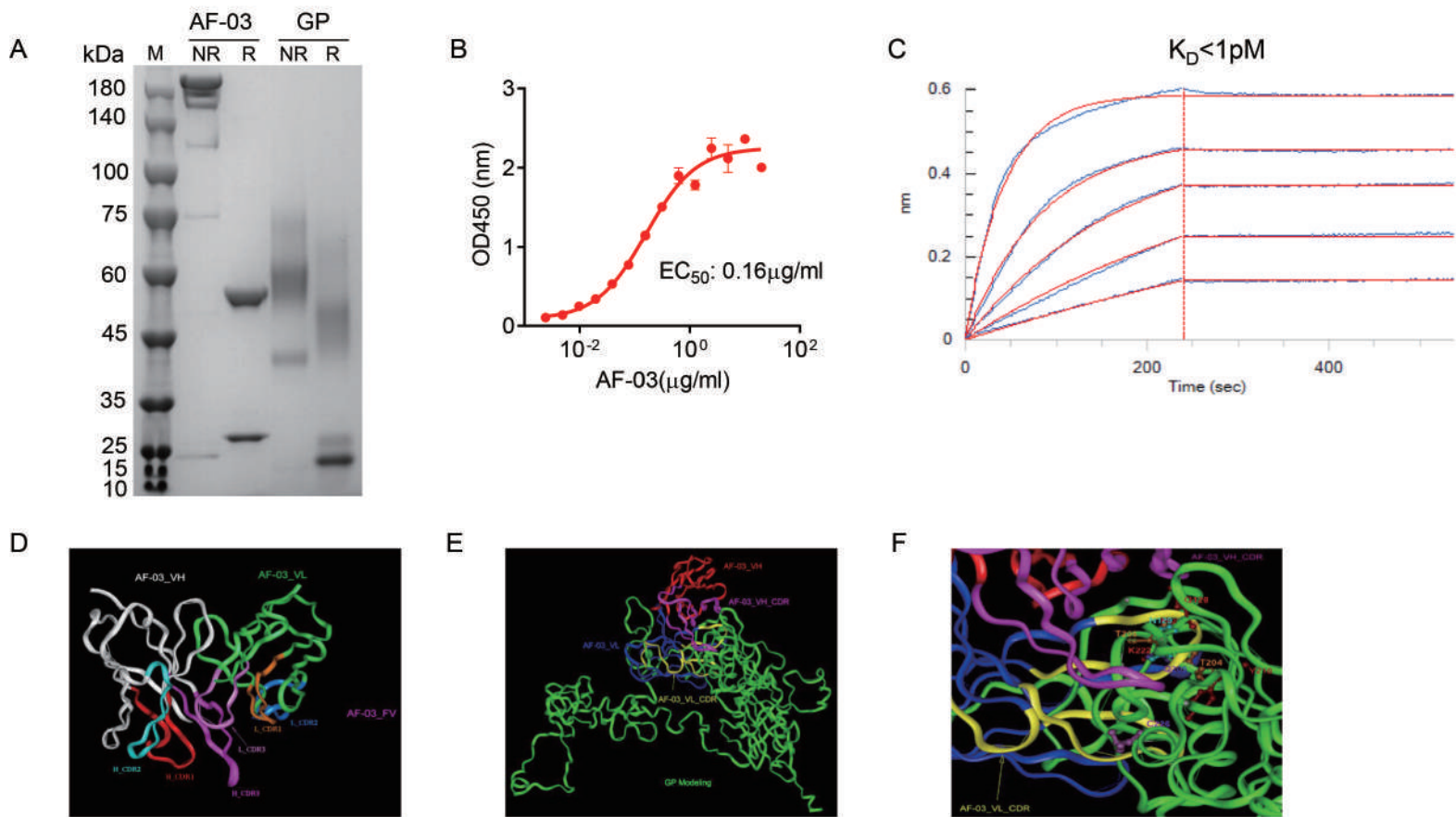
**Figure 6. Pan-filovirus entry inhibition by AF03-NL.**

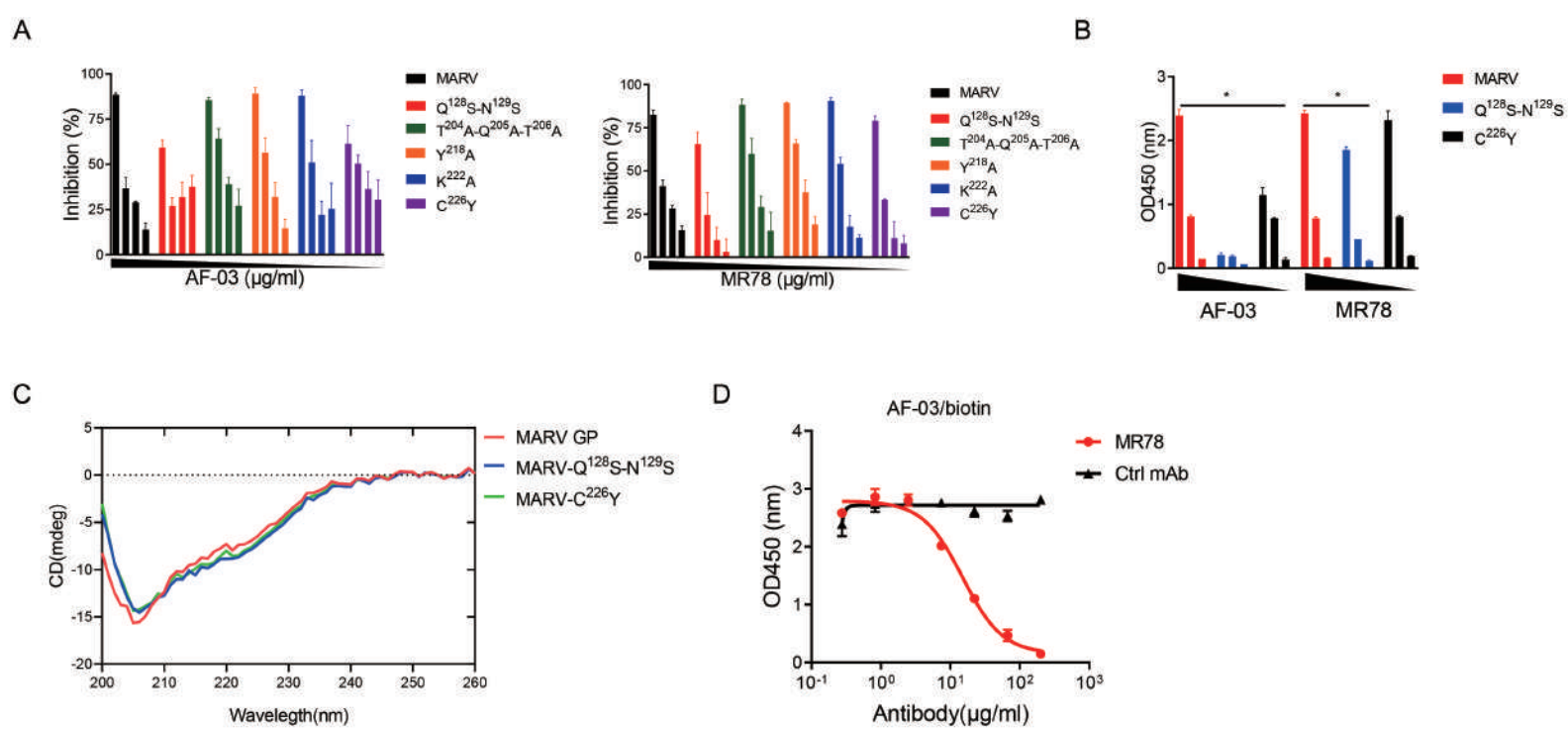
(A,B) AF-03 or AF03-NL is incubated with HEK293T cells at 37°C for 2 h prior to exposure to pseudotypic filovirus species (A) and EBOV mutants (B). Luciferase is assayed and inhibition rates are calculated.

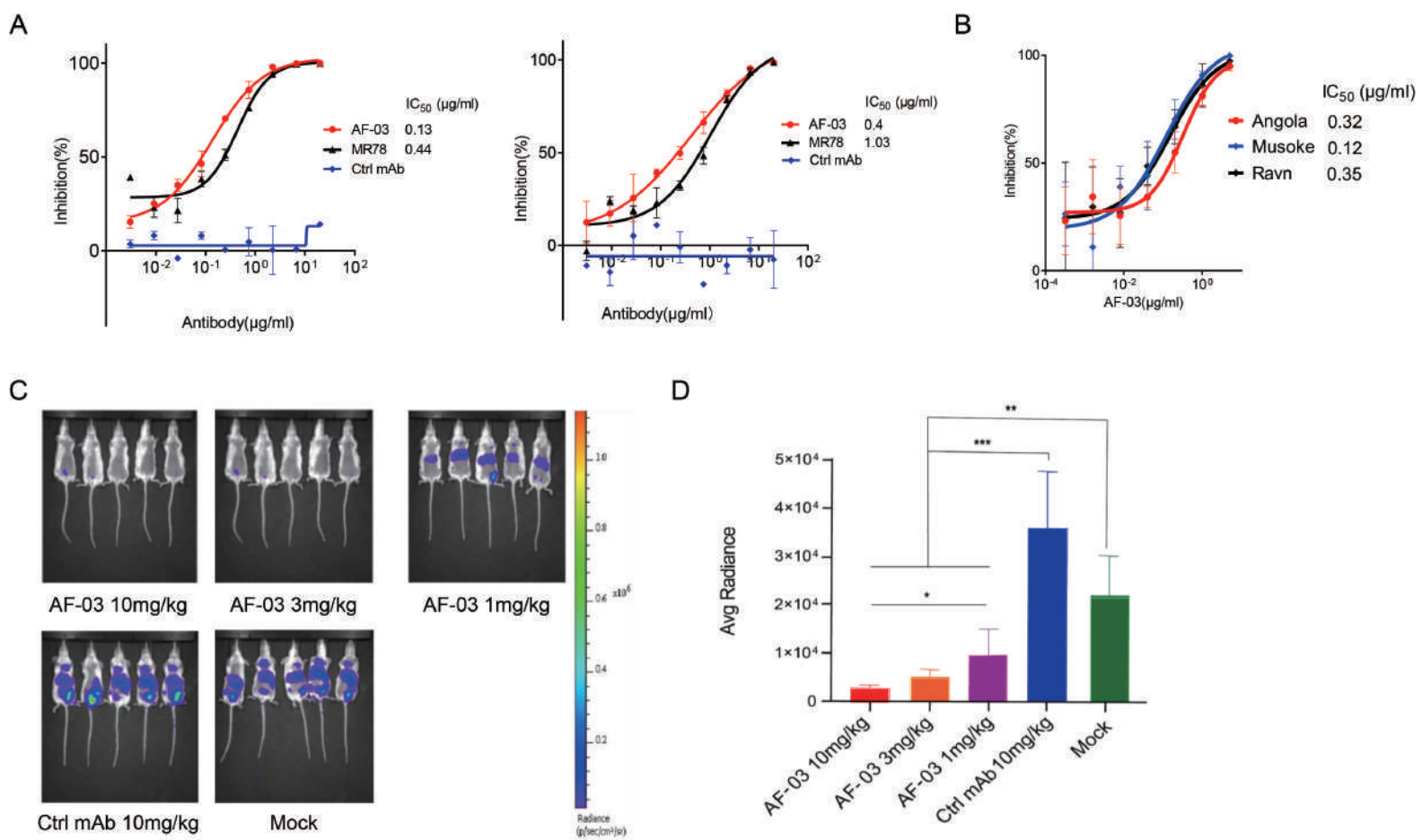
**Figure 7. The requirement of CI-MPR for the neutralization activity of AF03-NL.**

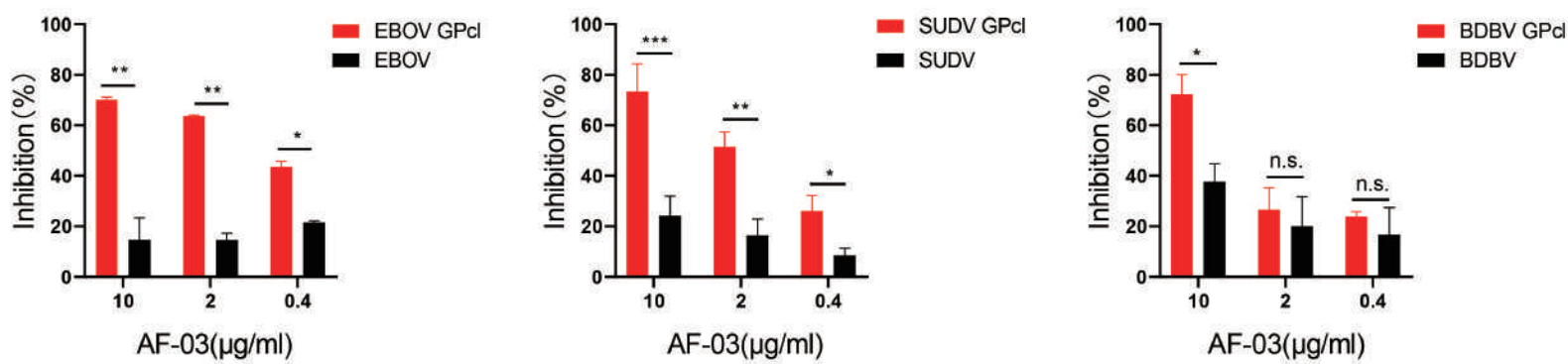
(A) NPC2 protein is examined by SDS-PAGE. NR, non-reducing; R, reducing. (B) AF03-NL, AF-03, NPC2 alone or equimolar combination of AF-03 and NPC2 is incubated with HEK293T cells at 37°C for 2 h prior to exposure to pseudotypic EBOV. Luciferase is assayed and inhibition rates are calculated. (C) HEK293T cells are treated with siRNA-CI-MPR or negative control vector (NC) respectively and CI-MPR expression is detected by flow cytometry. AF03-NL is incubated with

681 siCI-MPR or NC-treated HEK293T cells at 37°C for 2 h respectively prior to  
 682 exposure to pseudotypic EBOV. (D) CI-MPR is introduced into Huh7 cells and its  
 683 expression is detected by flow cytometry. AF03-NL is incubated with CI-MPR or  
 684 NC-knockin Huh7 cells at 37°C for 2 h respectively prior to exposure to pseudotypic  
 685 EBOV. Luciferase is assayed and inhibition rates are calculated.

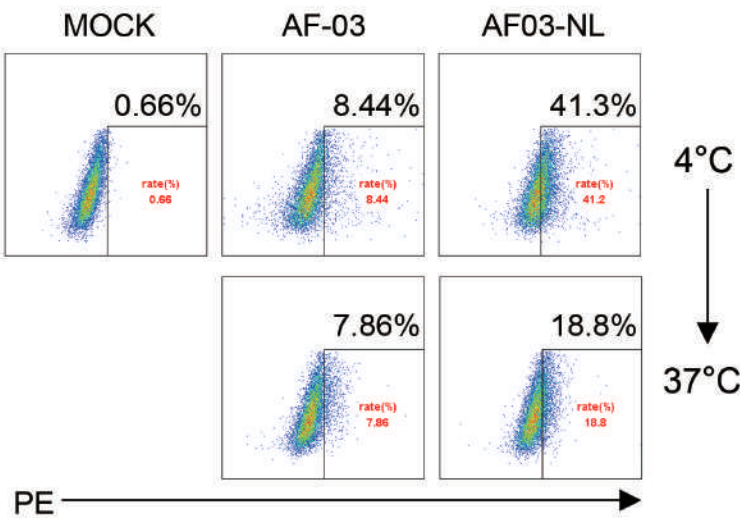




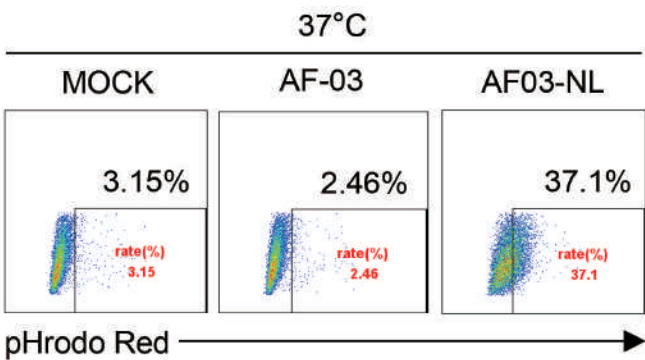




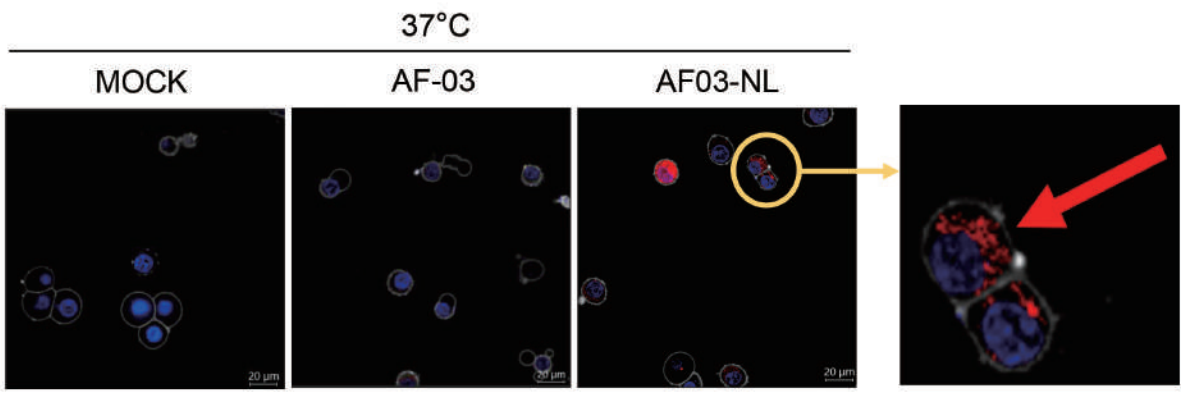
A



B

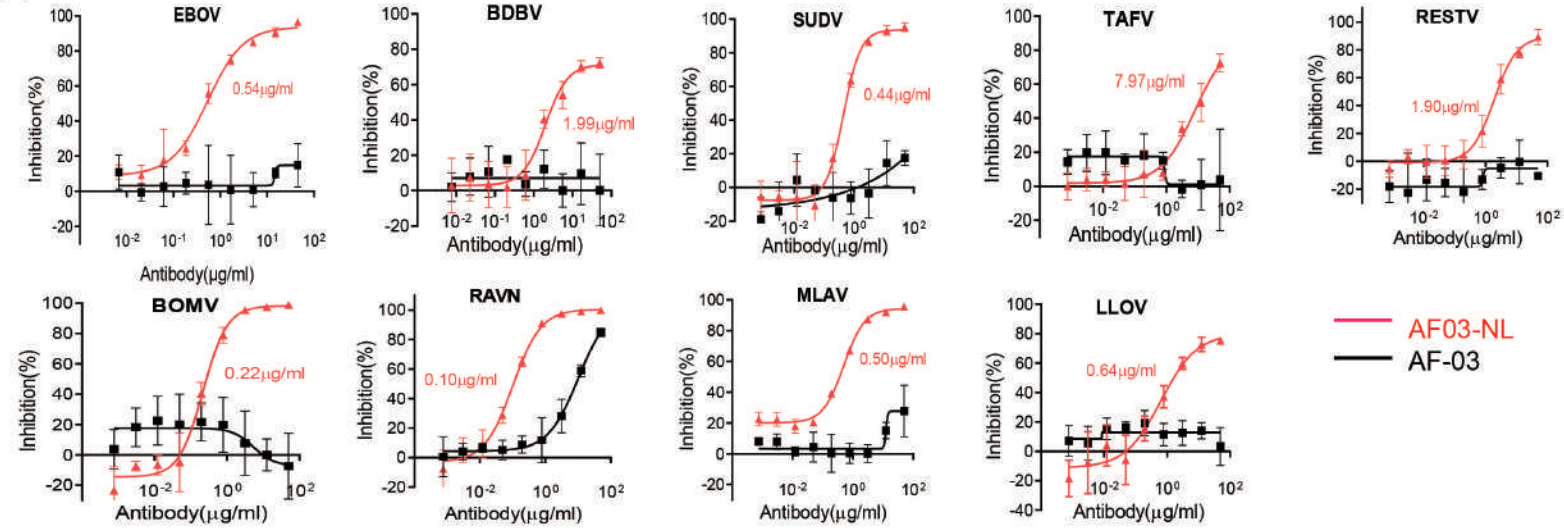


C

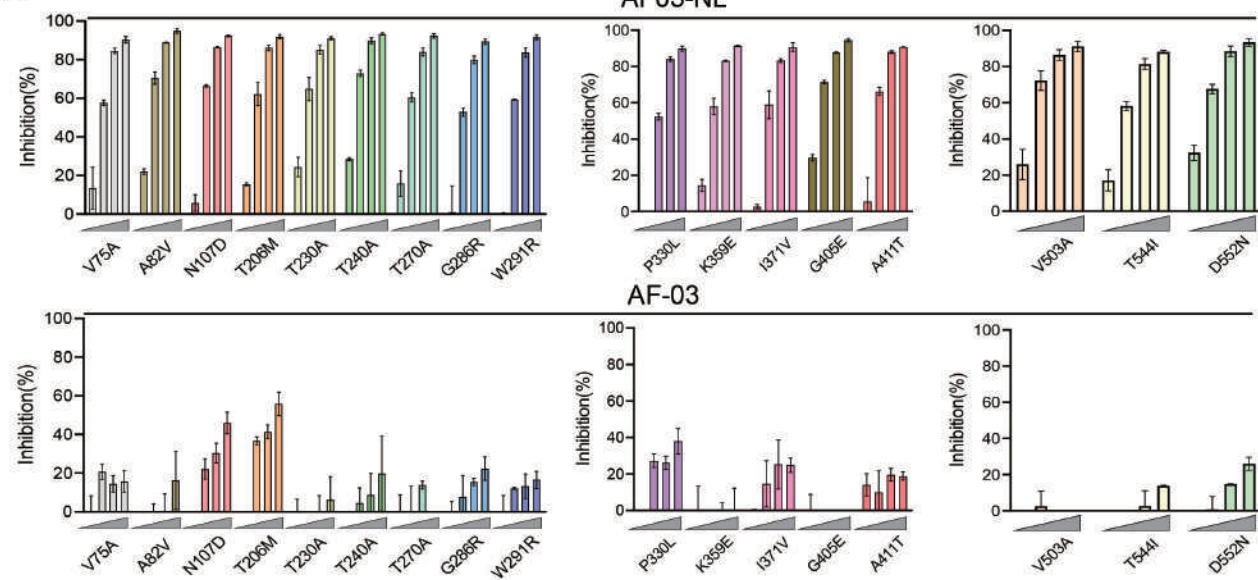




A

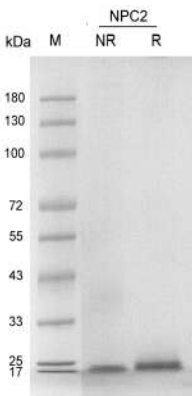


B

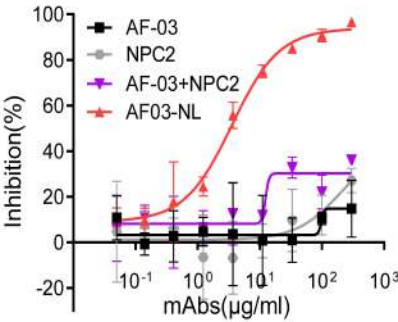




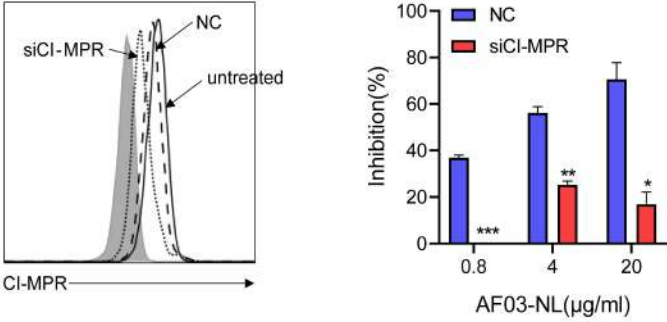
A



B



C



D

